A SEARCH FOR LATITUDINAL VARIATION IN SPACE WEATHERING ON MERCURY'S SURFACE.

Deborah L. Domingue[1], Faith Vilas[1], Pavel M. Trávníček[2], Mehdi Benna[3], David Schriver[4], and Menelaos Sarantos[5], [1]Planetary Science Institute, 1700 E. Fort Lowell, Suite 106, Tucson AZ 85719-2395 (domingue@psi.edu, fvilas@psi.edu), [2]Space Science Laboratory, University of California, Berkeley CA 90704 (pavel@ssl.berkeley.edu), [3]NASA Goddard Space Flight Center, Greenbelt MD 20771 (mehdi.benna-1@nasa.gov), [4]Institute of Geophysics and Planetary Physics, 3871 Slichter Hall, University of California, Los Angeles CA 90095-1567 (dave@igpp.ucla.edu), [5]Heliophysics Science Division, NASA Goddard Space Flight Center, Greenbelt MD 20771 (menelaos.sarantos-1@nasa.gov).

Introduction: Bombardment by charged solar wind particles has been shown to contribute to space weathering of planetary regoliths. Observations from the MErcury Surface, Space ENvironment, GEochemistry, and Ranging (MESSENGER) spacecraft during three Mercury flybys and in orbit about Mercury have indicated strong latitudinal variability in the surface flux of electrons, protons, and heavier ions. This variability raises the question of possible latitudinal variability in the spectral effects induced by space weathering on Mercury. With color imaging observations from MESSENGER's Mercury Dual Imaging System (MDIS) we are examining possible spectral variations that could be tied to space weathering processes induced by solar wind and magnetospheric ions.

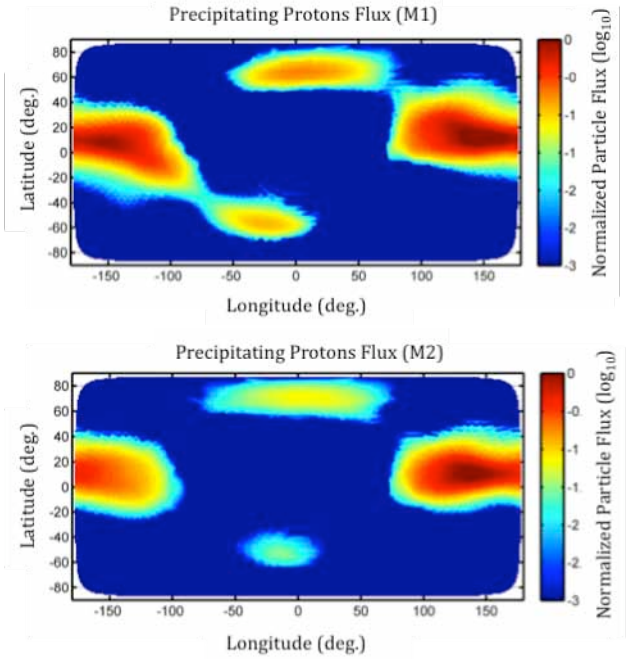

Fig. 1. Maps of precipitating proton flux onto the surface of Mercury during the first (M1, top) and second (M2, bottom) MESSENGER flybys modeled from Magnetometer measurements. 0° longitude corresponds to local noon. The fluxes are normalized to the flux of the undisturbed solar wind (9×10^8 particles/cm^2/s during M1 and 6×10^8 particles/cm^2/s during M2).

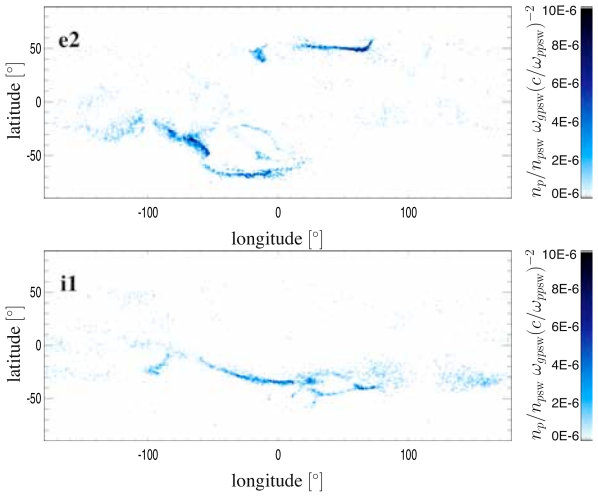

Fig. 2. Ion precipitation flux to Mercury's surface from a global hybrid simulation reflecting conditions observed in orbit by MAG and FIPS. In both simulations the IMF is oriented in Mercury's equatorial plane. The top pane shows results for sunward IMF, the bottom for anti-sunward IMF. 0° longitude corresponds to local noon.

Surface Particle Flux: Measurements taken by the Magnetometer (MAG) and the Fast Imaging Plasma Spectrometer (FIPS) on MESSENGER have been used to derive models of proton and electron precipitation flux to that planet's surface. The ion flux to the surface has been shown to be highly dependent on the orientation of the solar wind interplanetary magnetic field (IMF) [1]. For the first and second flybys (during which the orientation of the IMF was respectively northward and southward), models for the proton flux to the surface are shown in Figure 1. Ion precipitation flux to Mercury's surface obtained from hybrid simulations under different solar wind IMF orientations appropriate to orbit are shown in Figure 2. Studies of the magnetic cusp regions show that cusp properties depend on IMF orientation, and particle access to the surface can differ markedly between north and south [2]. The average area exposed to particle bombardment in the northern cusp is ~5.2×10^{11} m^2 compared with 2×10^{12} m^2 in the southern cusp region [2]. Particle fluxes are estimated to be ~1.1×10^{24} and 3×10^{24} particles/s in the northern and southern cusp regions, re-

spectively [2]. In each simulation, there is strong latitudinal variablitiy in the surface ion flux. Although these global precipitation patterns are strongly temporally variable, they show net latitudinal differences.

Imaging Data: Radiometrically calibrated and photometrically corrected (to incidence, emission, and phase angle values of 30°, 0°, 30°, respectively) color image sets were used to extract broadband reflectance spectra for several regions within the image frame. The regions selected included bright, younger units (such as crater rays or hollows) that are believed to be less space weathered than dark, older units (such as plains units). The spectral contrast between the different aged units were then examined as a function of latitude to seek any correlations.

Spectral variations have been indicated [3], although some calibration issues (such as scattered light, temperature, and read-out noise) remain under investigation [3] and may affect the magnitude and presence of some features.

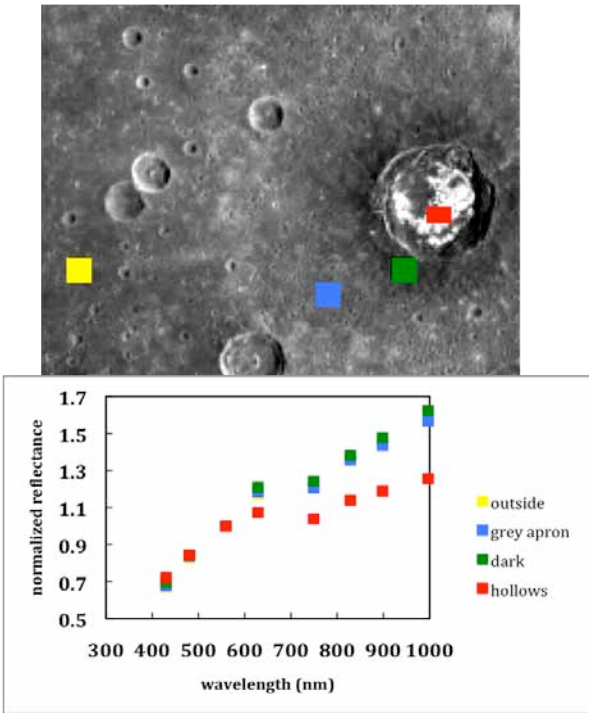

Fig. 3 Reflactance spectra are taken from a region associated with Sander crater (which contains hollows units in its interior) at 43° N, 154° E.

Preliminary Results: Comparisons were made of reflectance spectra from crater interiors and nearby plains (where the crater interiors are bright and younger than the adjacent plains). The crater regions studied to date were Kuiper (~10°N, 330°E) and Homer (~1°N, 323°E). The latitude difference in this comparison is small (~10°), and the spectral differences among the units appear similar between these two latitudes. Comparisons of hollows spectra (Figs. 3–5) with nearby units also show some spectral variations. All spectra shown are scaled to 1 at 556 nm and color coded to match the same colored regions in the images. The latitude difference in this case is ~39°. Although the differences might be compositional, they might also indicate differences in space weathering exposure. Additional pairs of units over a range of latitudes will be examined to see if a non-compositional trend can be established.

References: [1] J.A. Slavin et al. (2010) Science 329, 665 [2] R.M. Winslow et al. (2011) GRL, submitted. [3] F. Vilas et al. (2012) LPS 43, this meeting.

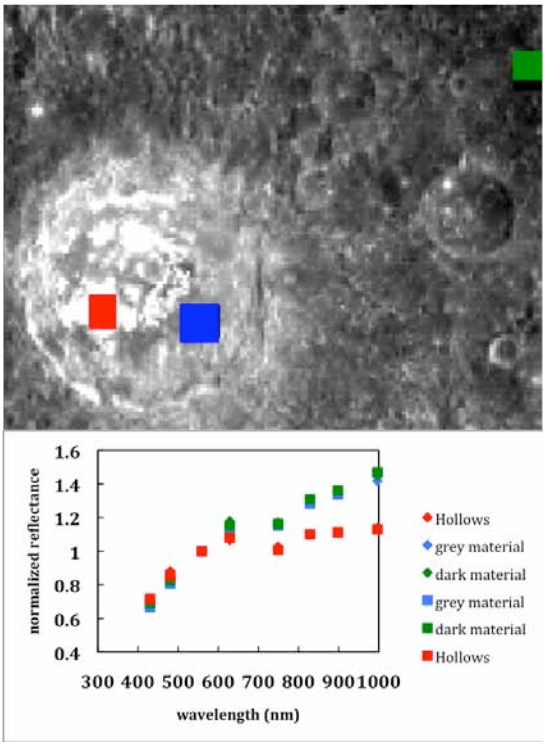

Fig. 4 Reflectance spectra are taken from a region associated with Tyagaraja crater (which contains hollows units in its interior) at 4° N, 210° E.

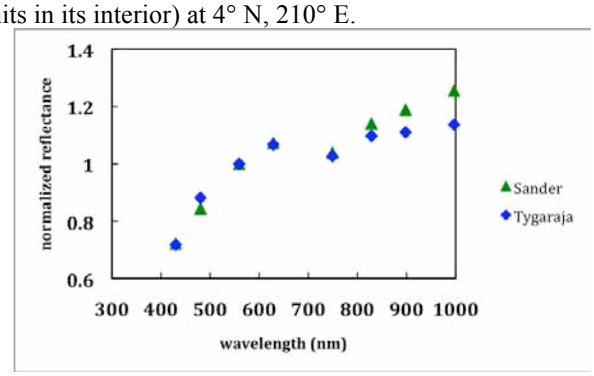

Fig. 5 Comparison of hollows spectra from 43° N (Sander) and 4° N (Tygaraja).